



OPEN ACCESS

EDITED BY

Sohail Mumtaz,
Gachon University, Republic of Korea

REVIEWED BY

Jamoliddin Razzokov,
Tashkent Institute of Irrigation and Agricultural
Mechanization Engineers (TIAME), Uzbekistan
Andrei Vasile Nastuta,
Grigore T. Popa University of Medicine and
Pharmacy, Romania

*CORRESPONDENCE

Samira Elaissi,
✉ saelaissi@pnu.edu.sa

RECEIVED 06 April 2025

ACCEPTED 07 May 2025

PUBLISHED 12 June 2025

CITATION

Elaissi S, Alsaif NAM, Moneer EM and
Gouadria S (2025) An analysis of
nanosecond-pulsed streamer discharges in
treating melanoma cells: generation,
source–plasma interaction, and energy
efficiency.

Front. Phys. 13:1606619.

doi: 10.3389/fphy.2025.1606619

COPYRIGHT

© 2025 Elaissi, Alsaif, Moneer and Gouadria.
This is an open-access article distributed
under the terms of the [Creative Commons
Attribution License \(CC BY\)](#). The use,
distribution or reproduction in other forums is
permitted, provided the original author(s) and
the copyright owner(s) are credited and that
the original publication in this journal is cited,
in accordance with accepted academic
practice. No use, distribution or reproduction
is permitted which does not comply with
these terms.

An analysis of nanosecond-pulsed streamer discharges in treating melanoma cells: generation, source–plasma interaction, and energy efficiency

Samira Elaissi*, Norah A. M. Alsaif, Eman M. Moneer and
Soumaya Gouadria

Department of Physics, College of Science, Princess Nourah Bint Abdulrahman University, Riyadh,
Saudi Arabia

Atmospheric pressure plasma has great potential in medicine, such as cancer therapy and wound treatment. Skin cancer therapy is challenging due to the thin layer of biological liquid covering the sample. This study aims to perform a numerical simulation of nanosecond high-voltage pulse plasma streamers applied to human tissue for melanoma cell therapy. This study investigates the optimization of plasma energy transfer in relation to several parameters, such as voltage, total energy, pulse frequency, flow rate, input power, and pressure. Results show that transient electric discharges can reach much higher electron energy levels than static discharges. As voltage increases, most reactive species' densities increase, and streamer length increases due to higher power deposition. In addition, as the pressure varies from 1 atm to 0.3 MPa, the breakdown time increases, and the propagation velocity of the ionizing front decreases. Pulse frequency affects thermal processes because contact time and input power of plasma increase with frequency. Due to a gradual cascade of biochemical processes that occur after treatment, melanoma cells often undergo apoptosis, resulting in slow cell death rather than necrosis, which occurs immediately. Melanoma cell death is most likely caused by the hydroxyl radical OH species produced from water vapor, which damages the outer surface of cancer cells through the oxidation process. Reactive oxygen and nitrogen species (RONS) like NO and O arising as primary products or metabolic byproducts have less influence. Based on these findings, it appears that these results are extremely important for treating cancer cells with non-thermal streamer discharge plasma.

KEYWORDS

atmospheric pressure plasmas, biological effects of plasmas, plasma–surface interface, pulsed streamer discharge, plasma oncology, apoptosis, modeling

1 Introduction

Various therapeutic plasma applications, such as treating infections, bleeding, healing wounds, tumor treatment, and dental decay, have been intensively studied over the last decades [1–3]. During plasma treatment, the human skin or culture medium is usually

dusted with a light blood layer, saline solution, or a serum liquid, bringing plasma into contact with a wet surface. Non-thermal plasma discharges have shown significant results in the treatment of diseases and the interaction with liquid systems [4]. Various cold atmospheric pressure devices have been produced for these purposes, such as dielectric barrier discharges (DBDs), plasma jets, streamer discharges, and glow discharges. Several sources have been used to evaluate the therapy mechanism and efficacy, including sinusoidal, radio frequency (RF), direct current (DC), pulsed DC, and microwave frequency [5]. DBD exhibits a non-equilibrium and quasi-continuous performance that generates a wide range of applications. DBD driven by pulse power offers more controllability of the discharge process and higher chemical efficiencies with lower gas temperature increases than alternating current (AC) or RF power DBD [6]. Fast transient pulsed discharges like streamers have the advantage of not being constrained by breakdown fields, producing a much higher electric field, and causing more electrical energy to be converted into energetic electrons, which contribute to plasma–chemical reactions [7]. Ionization can be further increased and electron energy distributions can be extended using short high-voltage pulses. A key difference between jet plasmas and most DBDs is the use of external feed gas [8]. Feed gas used in plasma jet experiments instantly necrotizes cells when directly in contact with the culture medium, even in plasma-off mode. As a result, a plasma jet with large gas fluxes typically requires enough liquid to prevent dehydration, even if part of the liquid is blown aside. Nevertheless, excessive liquids allow competing non-cellular targets to react with short-lived species, resulting in a dominant effect on the cellular functions of long-lived oxidants. On the other hand, a plasma streamer comes in contact with cells directly, simultaneously increasing the contribution of UV-radiation (low range), electrical fields, and short-lived species. Hence, nanosecond-pulsed streamer discharges have demonstrated their ability to create an equally diffuse, uniform, and highly reactive plasma as other standard plasma devices.

Non-thermal plasma streamer discharges generated by pulsed power are sources of high-energy electrons, ultraviolet rays, ozone, and free radicals in atmospheric pressure [5]. Hence, a thin layer of low-temperature, non-equilibrium plasma is formed and applied to a wet surface, which activates chemical reactions that affect cells, tissues, and bacteria without generating much heat [9–11]. The plasma species react with each other as well as with organic molecules present in the liquid layer prior to reaching the skin [12, 13]. Multiple timescales regulate the chemistry of these reactions in the plasma gas phase.

Various simulation models have been used to study the biological effect of plasma liquid. Kelly et al. [14] studied a radiofrequency plasma jet maintained in He/O₂ to generate a reactive surface on the liquid. A steady-state solution of a one-dimensional model was used to analyze plasma dynamics. Later, a 2D fluid and neutral chemistry model was used [15] to extrapolate the calculations of neutral plasma dynamics sources. The results of this study show that H₂O₂, O₃, O₂ (1Δ_g), and HNO₃ are the predominant RONS in the vapor layer, while H₂O₂(aq) dominates the RONS species in the liquid layer. Liu et al. [16] conducted extensive modeling research regarding micro-discharge on a liquid surface and defined three physical domains: plasma, gas containing neutral species, and liquids. A kinetics approach was used in

the plasma zone, while a 1D transport approach was used in neutral gases and liquids. Computationally, the strong coupling between all three regions allowed a simultaneous integration of all equations. The results showed that the potentially neutral species OH, NO, and O₂ (1Δ_g) transported from the distant plasma source to the liquid do not survive. Liquid chemistry was influenced by the gas phase species H₂O₂, O₃, HNO₃, and HNO₂, which produce dominant reactive species in the liquid, including OH(aq), allowing them to reach deeper depth in the liquid than the dominant reactive species generated from the remote source of plasma.

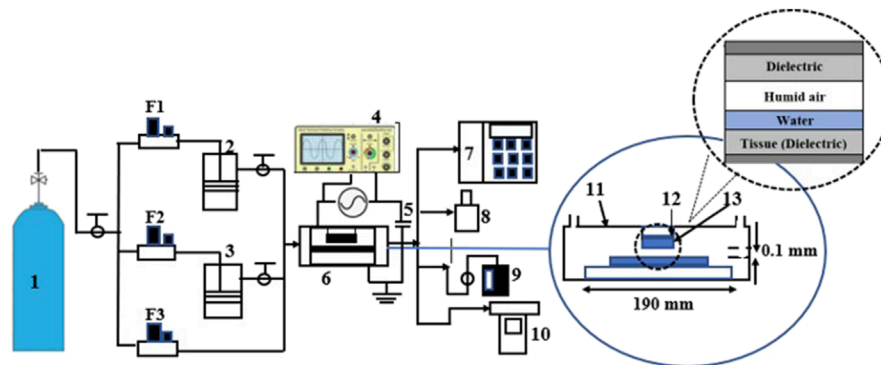
For optimal biological results, it is critical to examine how the gas phase is coupled to liquid chemistry and the effect of physical parameters on these processes. The objective of this research is to perform a simulation of a nanosecond high-voltage pulse plasma streamer applied to human tissue for melanoma cell therapy. A fluid model uses COMSOL Multiphysics® 5.1 with a two-dimensional axisymmetric geometry [17]. The field ionization mechanism and the morphology of the plasma channel are investigated in the gas phase under nanosecond voltage pulses. A parametric study of several operational conditions influencing plasma discharge and energy efficiency, such as voltage, input energy, pulse frequency, and pressure, is conducted. The effects of gas flow rate and oxygen concentration effects on plasma therapy are studied.

In this article, biomedical plasma processing is described in Section 2, and the simulation model is developed in Section 3. In Section 4, the results of this investigation are presented and analyzed. Finally, conclusions are summarized in Section 5.

2 General mechanism for biomedical plasma treatment

This study investigates a nanosecond-pulsed streamer discharge intended to treat melanoma cells. Recent research has demonstrated the efficacy of this method in skin cancer cell treatment [18, 19]. The experimental system used for biomedical plasma treatment, shown in Figure 1, includes an electrode system, an acrylic window with a plastic vessel to measure optical signals, and a cable input for inlet and outlet water [20]. A thin layer of serum or saline-like liquid is often applied to tissue during plasma treatment. Prior to reaching the underlying tissue, plasma species react with each other, as well as with liquid molecules and organic molecules in liquid. Water-dominated liquid systems have multiple timescales for reaction chemistry.

During gas-phase plasma pulses, the electron impact dissociations during the nanosecond plasma pulse produce oxygen atoms and hydroxyl radicals. Successive pulses are used to renew these species. Many species of reactive nitrogen are collected over several nanoseconds of discharge pulse [21]. Diagnostic methods are restricted to monitor concentrations of reactive species in liquids over hours or minutes of treatment [22]. The long-term chemistry of liquid plasma activation requires a large dynamic time range approaching several minutes [23].



1: Dry air cylinder, 2-water, 3-HCHO, 4-oscilloscope, 5-monitor capacitor, 6-reactor, 7-GC, 8-smart sensor humidity meter, 9-gas sampler, 10-aeroqual series 500, 11-PVC tube housing, 12- electrode and 13-aluminium oxide dielectric material. F1, F2 and F3 the flow rate meters.

FIGURE 1 Experimental setup of discharge plasmas for medical therapy.

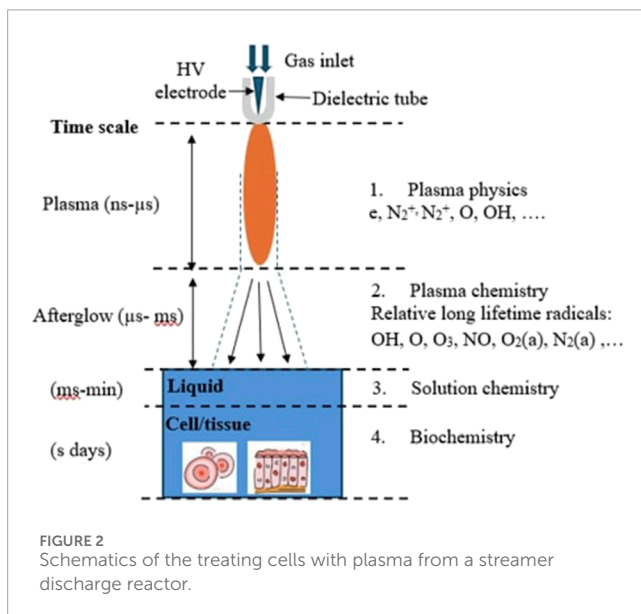


FIGURE 2 Schematics of the treating cells with plasma from a streamer discharge reactor.

3 Numerical procedure

3.1 Geometrical model

A schematic reactor diagram producing a high-energy streamer discharge is illustrated in Figure 2 [24]. A stainless-steel inner electrode with less than 10^{-3} m diameter is connected to a high-voltage cable. A generator with a variable number of stages generates high-voltage pulses with 10 kV charge voltage with 0.5–5 kHz frequency. The grounded electrode is constructed of stainless steel with variable diameters of approximately 40–88 mm. With a 2 mm air gap and a 1 mm water thickness, the geometry represents the treatment of a 1 cm^2 area of tissue.

3.2 Modeling equations

The streamer propagation in our study is modeled using Equations 1–10, which takes into account spatial and temporal variations in plasma particle densities. Several sources of plasma concentration are included in the plasma concentration equation, including electron drift, ambipolar diffusion, and term sources (electron impact ionization, three-body recombination, and dissociative recombination) [25]:

$$\frac{\partial n_i}{\partial t} + \text{div} \Gamma_i = k_i(E/N) n_1 N - \beta n_1^2 - \beta_3 n_1^3, \tag{1}$$

$$\Gamma_i = -D_i \nabla n_i + Z_i \mu_i n_i E, \tag{2}$$

where n_i denotes the density of different species i (electrons, positive ions, and negative ions), Γ_i denotes electron flux, D_i is the coefficient of diffusion, and μ_i represents the mobilities of the charged species. The diffusion coefficients and the drift coefficients are calculated from the Einstein relation.

$k_i(E/N)$ represents the rate of ionization; β and β_3 are constants of dissociative recombination and three-body recombination, respectively.

To determine the electric field strength, conductive and displacement currents should be considered [26].

$$\text{div}(\mathbf{J}) = 0, \tag{3}$$

$$\mathbf{J} = \left(\sigma + \epsilon \epsilon_0 \frac{\partial}{\partial t} \right) \mathbf{E}, \tag{4}$$

where σ conductivity $\sigma = e \cdot \mu_e \cdot n$ (for gas) and $\sigma = 0.5, 600 \mu\text{S}/\text{cm}$ (for barrier dielectric or water); ϵ_0 represents the free space permittivity, and ϵ denotes the dielectric permittivity.

The total current is continuous at the intersection of two media, assuming the dielectric or conducting barrier has a negative charge on its surface. Differences in normal electric

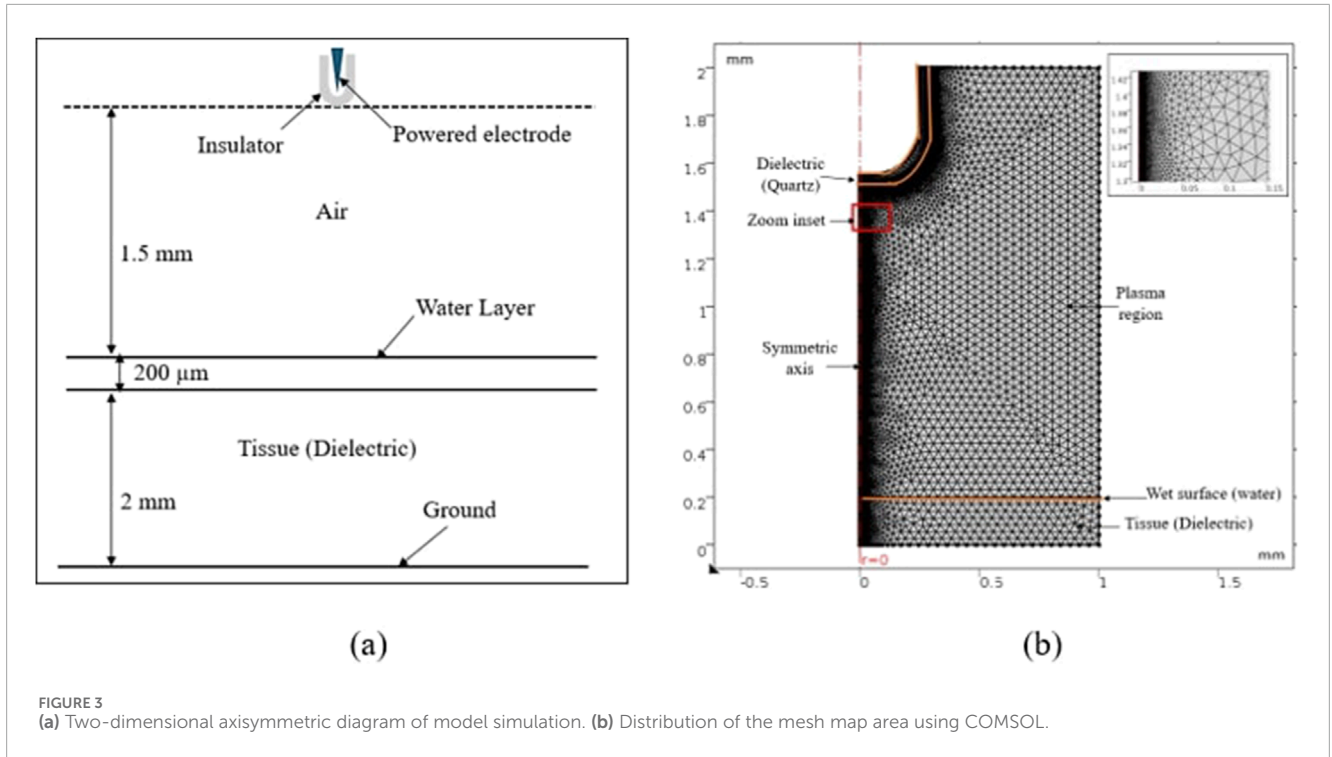


FIGURE 3 (a) Two-dimensional axisymmetric diagram of model simulation. (b) Distribution of the mesh map area using COMSOL.

displacement fields on two sides of a barrier surface are calculated as surface charges:

$$q_s = \epsilon_0(\epsilon \cdot E_b - E_{air}), \tag{5}$$

where the electric field is determined as

$$E = -\nabla \cdot V. \tag{6}$$

A potential $V = 0$ is used at the grounded electrode as a boundary condition, while the cathode potential V_{cat} can be calculated as

$$V_{cat} = V_0(t) - V_R, \tag{7}$$

where $V_0(t)$ represents the pulsed source voltage, and V_R is the resistance voltage on the external circuit calculated as

$$V_R = R \cdot J_{SUM}. \tag{8}$$

Over the grounded electrode, the vertical component of the current density J_y is integrated to determine the total discharge current as follows:

$$J_{SUM} = \int J_y(x) dx. \tag{9}$$

The initial gas composition is the humid air and consists of 80% N_2 , 17% O_2 , and 3% H_2O mixture gas considering water evaporation [27]. A high pulsed 10 kV voltage is applied to the powered electrode with a rectangular signal which has a pulse width of 10 ns, a decreasing or increasing time of 0.8 ns, and a frequency of 1 kHz to ensure a homogeneous discharge with safe treatment of an irregular, dirty, and wet surface of living tissue. The initial electron density is introduced as [28]

$$n_e(r, z)_{t=0} = n_{e,0} \exp \left[-\left(\frac{r}{\sigma_r} \right)^2 - \left(\frac{z - z_0}{\sigma_z} \right)^2 \right] + n_0, \tag{10}$$

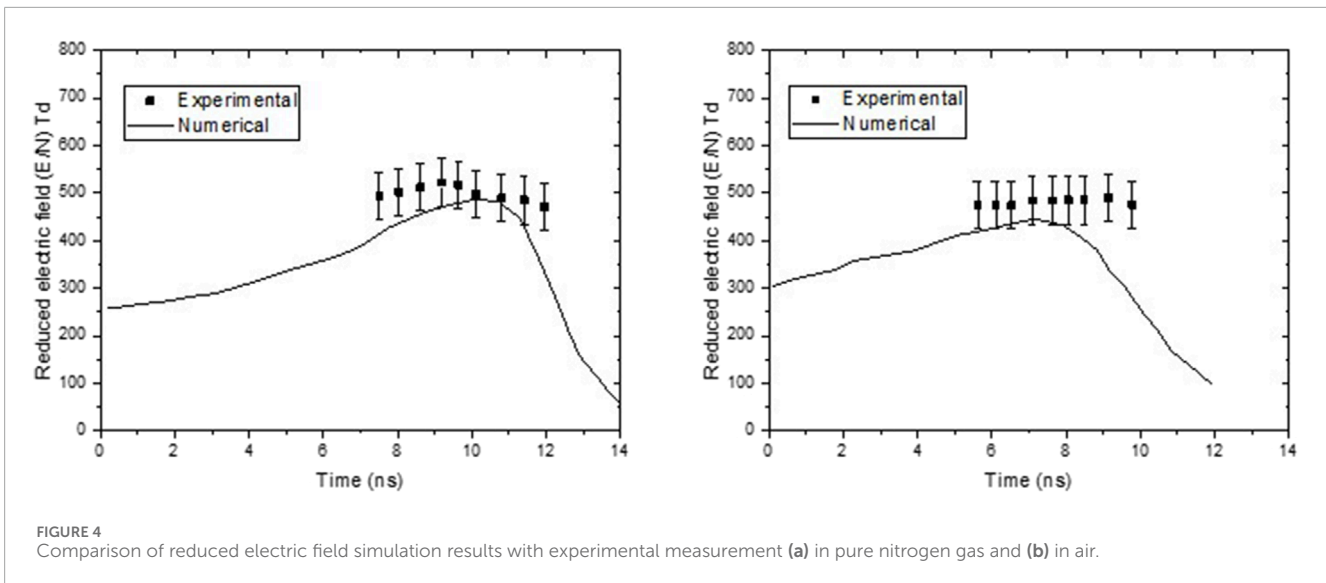
where $n_{e,0} = 10^{18} \text{ m}^{-3}$; $n_0 = 10^{10} \text{ m}^{-3}$; $\sigma_z = \sigma_r = 0.07 \text{ mm}$; and $z_0 = 1.5 \text{ mm}$ at $r = 0$. A constant 300 K room temperature is assumed for the plasma air gap and water layer.

3.3 Computational modeling

Streamer discharge simulations are conducted using COMSOL Multiphysics commercial software [29]. A pin plate electrode arrangement is investigated, as shown in Figure 3a. This design is characterized by a pin tip with a 0.2 mm radius and a 1.3 mm gap distance between the pin and the plate. The applied area employed to calculate simulated plasma parameters is $r \times z = 1 \times 2 \text{ mm}^2$. Different meshing densities using the finite element method are required for accuracy and stability because the streamer is mainly concentrated near the axisymmetric line, where the discharge is occurring and the electric field gradient is extremely high. The numerical calculations are greatly improved by using an extremely fine mesh structure near the symmetrical axis. Figure 3b shows different fine grids applied near the symmetry line that divides the simulation area. The inset in Figure 3b illustrates the zoom of meshes and the accuracy of enlargement of certain meshes.

4 Results and discussion

The initiation and development of the streamer are studied using a discharge process at atmospheric pressure (0.1 MPa) in a plasma gap of 1.3 mm containing a nitrogen, oxygen, and water vapor mixture and with a pulsed voltage amplitude of 10 kV (the pulse has the characteristics of 10 ns width and 0.8 ns rise time). Then, the



results are discussed according to various operational parameters, including pulse frequency, voltage, and flow rate of gases.

4.1 Validation

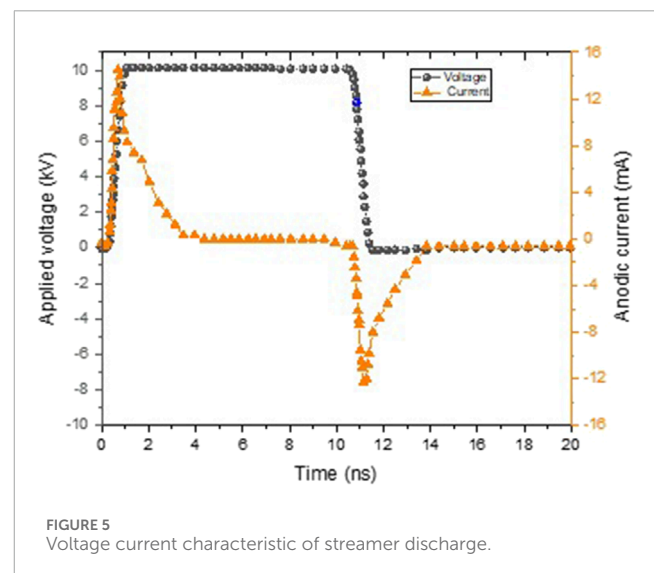
The numerical results are compared with experimental measurements to prove their accuracy. In Figure 4, the numerical and experimental reduced electric fields are presented for pure nitrogen and in air. Numerical results agree well with experimental data performed using photo multipliers [30].

4.2 Characteristics of streamer discharge

Figure 5 shows the current and voltage distribution. A streamer corona discharge is produced by applying 10 kV to the high-voltage electrode. Streamer current is characterized by a fast pulse current of 14 mA at a frequency of 1 kHz [31], producing a non-thermal plasma of 300 K.

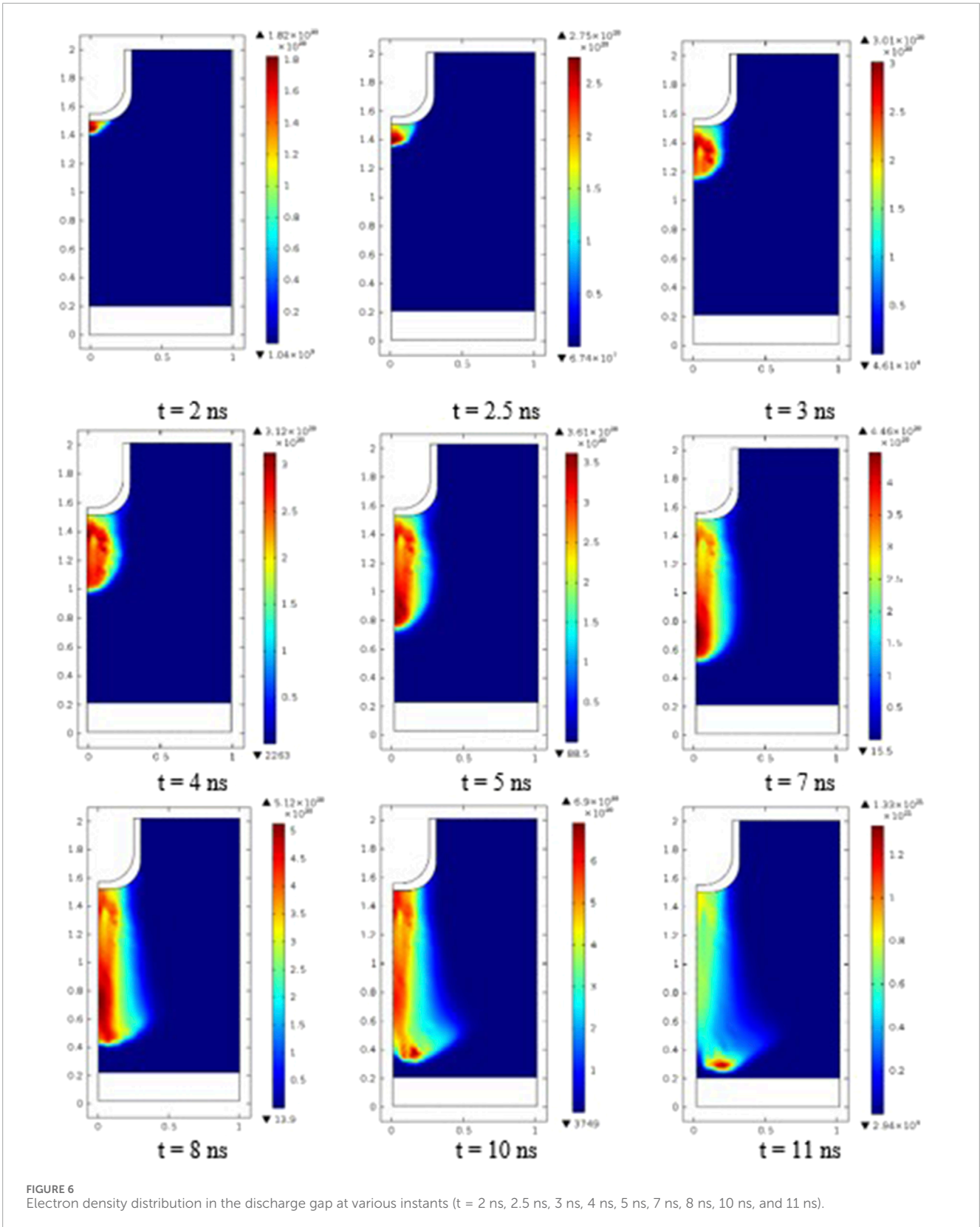
The plasma is highly capacitive and is dominated by displacement current. A high-energy deposition per pulse for the positive polarity is gained and can be calculated by integrating the product of the current and voltage waveforms over time. This is in accordance with previous results obtained by Van Doremale [32], who demonstrated a higher charge deposition on the substrate using positive polarity.

Figure 6 represents the evolution of the electron density at various instants, which supports understanding the morphology of the discharge and of the different processes occurring from the needle tip toward the ground electrode. When the voltage attains 10 kV, the streamer creates a conductive channel that forms a spark. Indeed, the local gas heating causes a decrease in the gas density N . This enhances the reduced electric field (E/N) associated with the streamer-induced channel. A spark breakdown with higher current pulses occurs because E/N controls electron impact reaction, in particular ionization [33]. A restricted spark



pulse current emerges, and the voltage drops with increasing current. The sparks are only transient when they form due to small energy discharge. New pulses are triggered in response to the growing potential at the stressed electrode. One or more streamer pulses precede each spark pulse, resulting in an endless streamer-to-spark discharge. The small pulse duration, depending on the frequency (0.5–5 kHz), prevents the plasma from reaching local thermodynamic equilibrium and maintains the gas at a low temperature.

Figure 7 shows the distribution of the charged and neutral species density in humid air. As shown in Figure 7a, neutral species like O_3 and NO accumulated in the gas over several pulses; however, the other neutral species are depleted with each pulse. RONS accumulate at the surface liquid and then decline during the post-plasma period. Liquid pH decreases as a result of the presence of HNO_x acids generated in the gas and dissolved in the liquid. Figure 7b shows that negative ions are influenced by



the accumulation of neutral species and evolve over many pulses, while positive ions are not significantly affected. In Figure 7c, the propagation and diffusion of various RONS across the

plasma–liquid interface, along with the approximate timescale governing various phenomena across the plasma–liquid phases and biological interactions, are described.

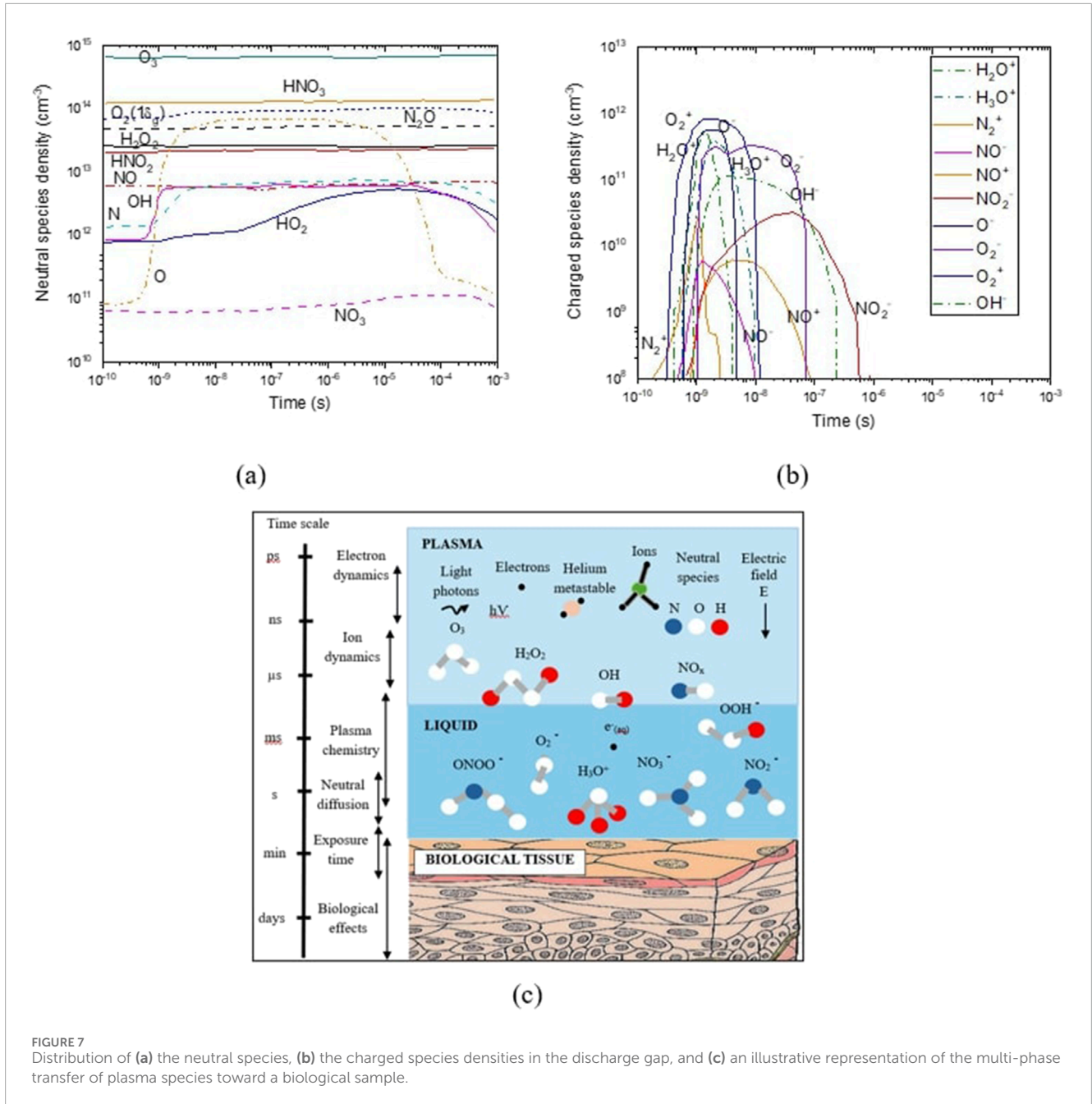


FIGURE 7 Distribution of (a) the neutral species, (b) the charged species densities in the discharge gap, and (c) an illustrative representation of the multi-phase transfer of plasma species toward a biological sample.

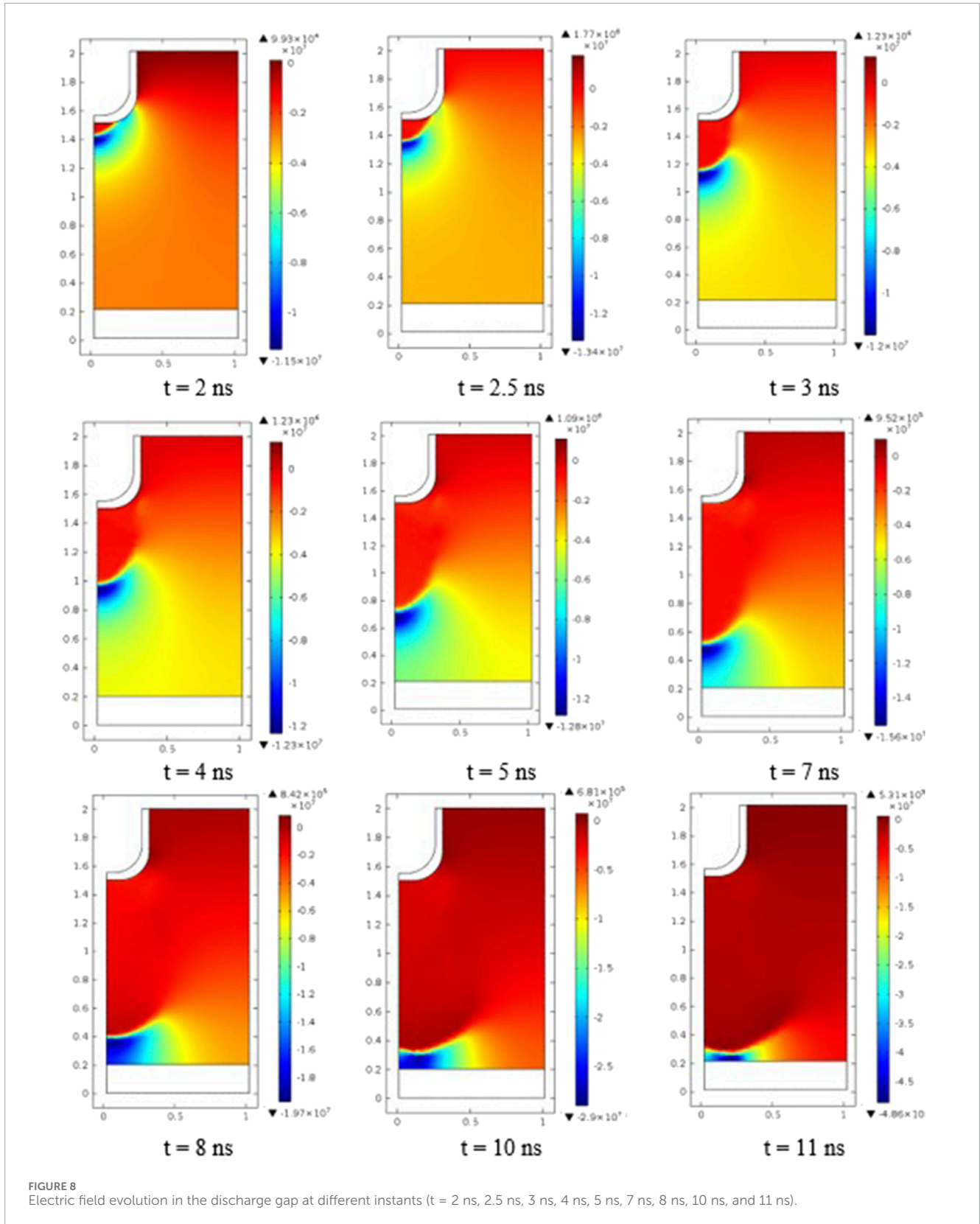
Figure 8 shows the electric field distribution at various instants of applied voltage. The maximum electric field intensity occurs at the needle tip because it has the smallest radius of curvature. After several nanoseconds, the electric field in the vicinity of the electrodes becomes inhomogeneous, resulting in the occurrence of the ponderomotive force, which acts on the plasma medium and directs itself to the grounded electrodes [34].

The discharge dynamic is determined by the current continuity, and the displacement current is converted into the convection current inside the plasma [35]. Upon reaching the cathode, a glow discharge with a voltage drop and a constant value of the electric field of approximately 531 kV/m ($t = 1,100$ ns) is established in front of the cathode. There is a slow radial expansion of field enhancement.

4.3 Insensitivity to simulation parameters

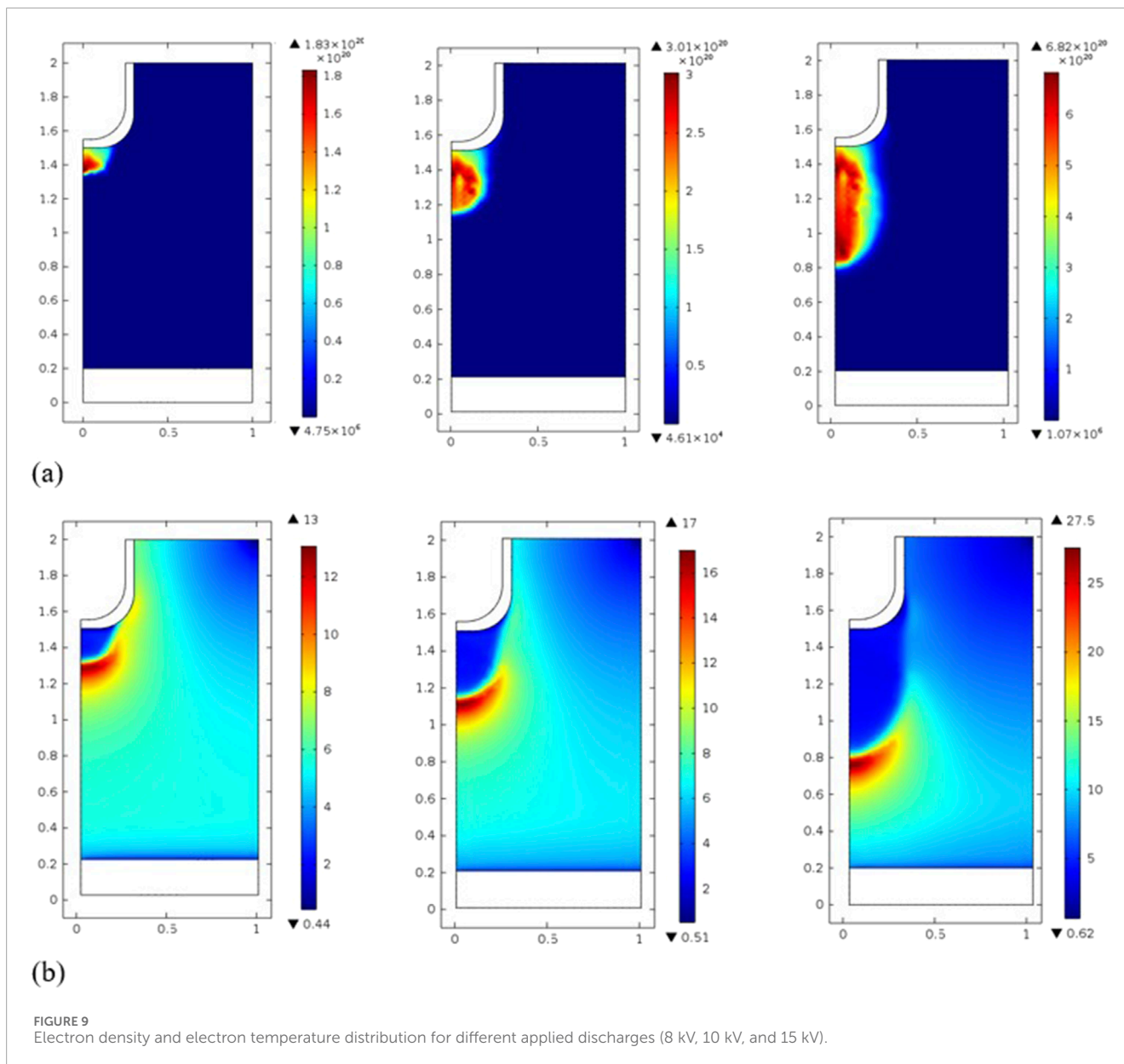
4.3.1 Influence of applied discharge

Voltages ranging from 8 to 15 kV are applied in a parametric study, as shown in Figure 9. Due to the greater energy deposition at higher voltage, the density of most species increases. A change in maximum electron density occurs from $1.83 \times 10^{20} \text{ m}^{-3}$ at 8 kV to $6.82 \times 10^{20} \text{ m}^{-3}$ at 15 kV, as well as an increase in electron temperature from 13 V to 27.5 V. Because of the gap's short diffusion length, the peak gas temperature is kept low primarily by thermal conduction, and all cases show a peak temperature below 303 K. The temperature difference of 3 K in a 1.2 mm gap is sufficient to conduct an energy flux into the walls in 10 ns because the contact surfaces are maintained at 300 K [36].



As shown in Figure 10, the streamer length rises with applied voltage from 8 kV to 25 kV. Hence, the streamer propagates further at higher voltages due to the increase in expansion velocity with the

voltage amplitude. The homogeneity of the streamer is reduced with the increased applied voltage, and the streamer is less constrained along the axial axis with several branches.



4.3.2 Influence of input power

In discharge plasma input, power plays a crucial role in degrading cancer cell activities and killing them, where the increase in input power enhances the medical therapy [37]. In fact, higher input power is associated with a higher electron density in the reaction medium, resulting in the production of many reactive oxygen species, including O_3 , OH , and O , which contribute to the degradation of microorganisms [38, 39]. By increasing input power, electric fields allow electrons to gain more energy, thus causing further ionization of oxygen and H_2O molecules [40]. Then, higher energy density means more energy can be stored and released.

The power density shows the acceleration of the quantity of energy provided for a limited period of time. Higher power density also signifies a faster charge/discharge rate, which can result in more energy being recovered [41]. Figure 11 shows that the streamer length rises with increasing energy input [42].

4.3.3 Influence of pressure

The streamer's structure and velocity studied in a nanosecond time scale are greatly affected by applied pressure. As shown in Figure 12, the speed at which an ionizing front propagates declines with pressure [43]. Hence, there is a decrease in the volume and number of streamers in response to increased pressure [44].

Furthermore, the breakdown time increases as the pressure changes from atmospheric to 0.3 MPa. If the pressure is increased further, the streamer will disappear, along with the currents and light pulses associated with it. However, when pulse durations are reduced to sub-nanosecond levels, pressure influence decreases [45].

4.3.4 Influence of pulse repetition frequency

Two distinct modes of pulsed plasma discharge are generated by increasing the pulse frequency from 1 kHz to 10 kHz [46]: (i) the

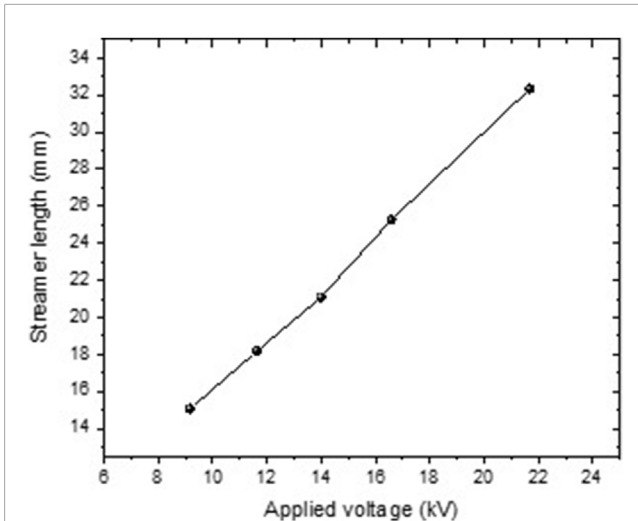


FIGURE 10 Variation of streamer length with applied voltage.

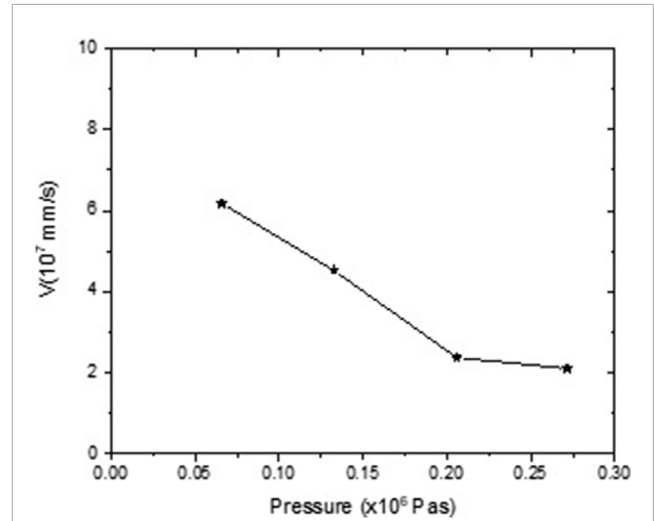


FIGURE 12 Variation of the velocity of ionizing front streamer with pressure.

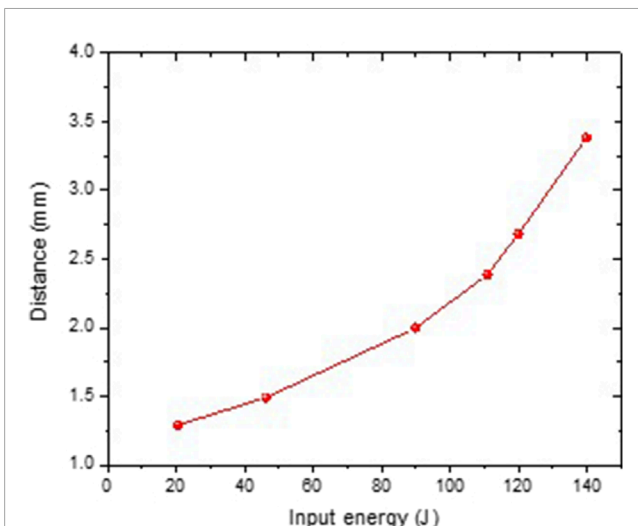


FIGURE 11 Variation of energy input into streamer discharge with interelectrode distance at various applied voltage pulses.

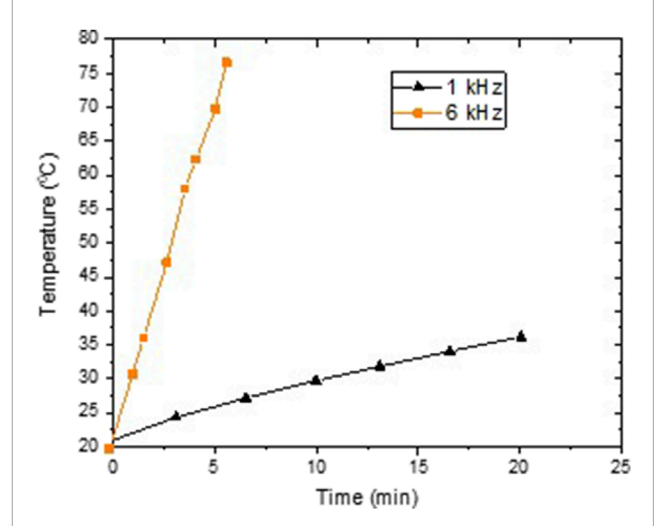


FIGURE 13 Temperature variation during the discharge plasma treatment using high-voltage pulses with the frequency of 1 kHz and 6 kHz.

first mode is a streamer mode, where a corona discharge propagates through a streamer channel, and (ii) the second mode involves a rise in pulse repetition rate which reduces the streamer channel and suppresses the streamer mode when exceeding a threshold value, usually 10 kHz.

With varying pulse frequencies, several effects contribute to the change of plasma morphology. Indeed, increasing pulse frequency changes thermal processes due to an increase in power input and time of plasma contact. Figure 13 illustrates the increase in temperature caused by high-voltage pulse discharge of 10 kV at 1 kHz and 6 kHz. A discharge operating at an elevated pulse frequency heats the tissue to a higher temperature faster. A discharge at 6 kHz increases the water temperature by more than 50°C within 5 min, while this magnitude of temperature gradient is not

observed at lower frequency discharges. Using 1 kHz only increases temperature by 10°C [47].

4.3.5 Influence of the flow rate

Discharge plasma treatment technology greatly depends on the quality and quantity of input gases. The degradation of microorganisms is more efficient in oxygen than in air gas [48]. An analysis of the effects of oxygen concentration and gas flow rate with pulsed streamer discharge is presented in this study. The densities of O, NO, and OH, which play a crucial role in plasma medicine, are displayed to analyze the correlation between cell death and reactive species on the growth medium. A variety of reactive species are generated in liquid from OH and NO radicals [49,50], and atomic oxygen is a powerful oxidant with significant biological effects.

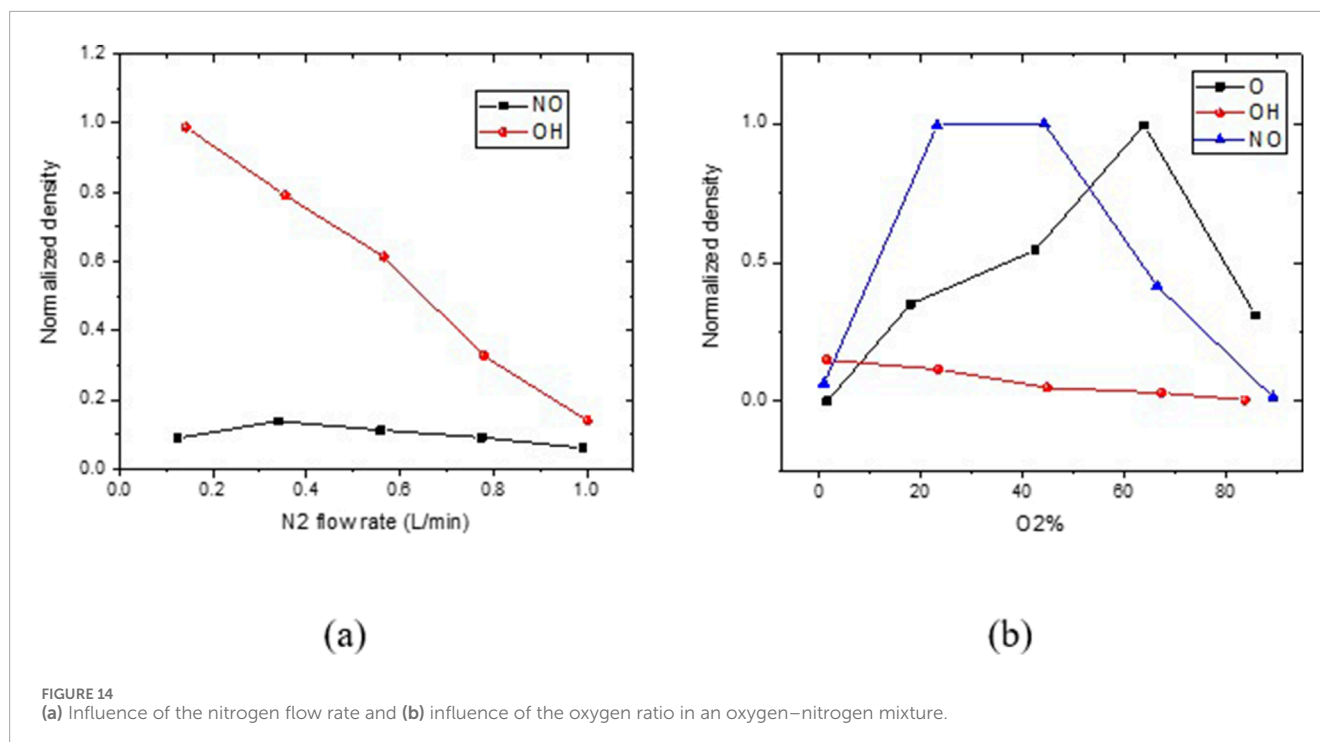


FIGURE 14
(a) Influence of the nitrogen flow rate and (b) influence of the oxygen ratio in an oxygen–nitrogen mixture.

Figure 14a shows that when ($O_2 = 0\%$) and as the N_2 flow rate increases, OH density declines by diluting it because of the existence of water vapor concentration, which is necessary to produce OH radicals. Hence, the increase in the N_2 gas flow rate reduces the cell death rate and decreases the efficiency of microorganism removal by generating fewer reactive species. The degradation efficiency does not improve beyond a certain gas flow rate, and the decrease in NO concentration at the system outlet confirms these results [51].

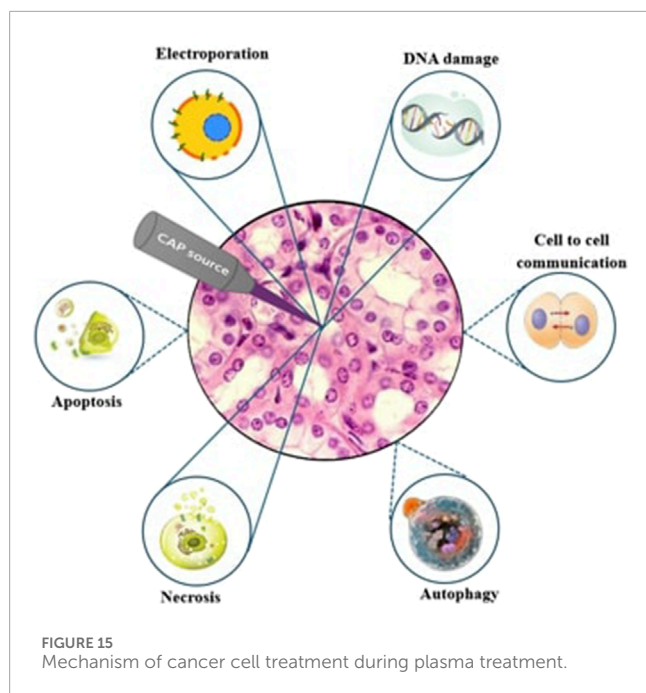
As shown in Figure 14b, the O_2/N_2 discharge does not affect cell death despite a considerable increase in O_2 concentration with a constant flow rate. Based on these findings, it appears that melanoma cell death is most likely caused by OH, which is a reactive species that is derived from water vapor. Oxygen-derived reactive species like NO and O have little influence because they emphasize the significance of incorporating water evaporation into the culture medium [52].

4.4 Correlation analysis

Rather than being removed by short-lived reactive species, melanoma cells are removed by long-lived chemical species dissolved in the medium. Long-lived chemical species interacting in cell death are reactive oxygen species (HO_x), reactive nitrogen species (HNO_x), and organic substances created when organic compounds react with reactive gas species [53]. According to Figure 14, OH radicals' flux to the medium surface results in cell death. Indeed, OH radicals are precursors of subsequent chemical reactions that result in the removal of cancer cells. H_2O_2 is one of the long-lived chemical species that removes cancer cells [54]. The flux of short-lived species in the medium has

an important correlation because it initiates the death process in cells [55].

Initially, reactive plasma species interact with the transmembrane proteins and membrane lipids [56]. Cell membranes are initially oxidized or modified by plasma species. During lipid oxidation, the membrane permeability is increased, lipid mobility in the phospholipid bilayer (PLB) is altered, pores are created, and the bilayer disintegrates [57]. The fluidity and stability of cell membranes are maintained by cholesterol, which is typically low in cancer cell plasma membranes. Hence, the formation of pores allows reactive species to easily enter cancer cells, explaining how plasma treatment targets cancer cells. In addition, aquaporins (AQPs) act as transport channels for H_2O and small reactive molecules like NO, NO_3^- , and H_2O_2 [58] across the membrane. A higher number of AQPs are found in the cytoplasmic membrane of cancer tissues than in homologous normal tissues, explaining why cancer cells are more susceptible to plasma therapy. A variety of nitration products are formed by reactive nitrogen species (RNS) interacting with the membrane, including nitro phospholipids. Nitrated lipids are produced from this process in high yields, similar to lipid oxidation. Nitrated membranes are three times more permeable to water than oxidized membranes due to the impact of nitration. Reactive species generated by plasma can penetrate cell membranes. Compared to normal cells, cancer cells have a noticeable increase in reactive oxygen species (ROS), increasing oxidative damage to biomolecules. Cell death must also be activated by the apoptosis mechanism. Along with RONS generation, plasma sources also generate strong electric fields, which play a synergistic role in plasma–cell interaction, as they can temporarily or permanently electroporate membranes [59]. Mitochondria are irreversibly damaged by repeated electric field shots. Moreover, short electrical pulses can trigger apoptosis in cells. Cells can be selectively killed using electrical pulses.



Consequently, when melanoma cells receive plasma treatment, they often undergo apoptosis rather than necrosis [60]. Due to a gradual cascade of biochemical processes, apoptosis induces cell death that takes some days. In contrast, necrosis occurs instantly following plasma treatment [61]. So, apoptosis mainly induces slow cell death, and the survival rate does not decrease rapidly after treatment.

Our results aligned well with the experimental study of Biscop et al. [62], who emphasized an increase in caspase 3/7 and annexin V expression, indicative of apoptosis, as well as lipid peroxidation, characteristic of ferroptosis, following both direct and indirect NTP treatment of melanoma cells. Furthermore, Arndt et al. [63] investigated the effects of surface micro-discharge technology on melanoma cell treatment. They affirmed that in response to different CAP doses, tumor cells induce apoptosis or senescence differently.

Finally, plasma medicine could be considered more effective than chemical radiation therapy because it considers short-lived reactive species, charges, densities, electric fields, and their synergetic effects, as well as long-lived species [64]. As shown in Figure 15, the immediate vicinity of an ignited plasma creates reactive species that cause necrosis, DNA damage, and potentially electroporate effects on cells. The diffusion of longer-lived species into the tumor periphery contributes to the induction of apoptosis. Plasma source proximity is used to estimate the effects and responses of cells.

5 Conclusion

This research examines the biological assessment of plasma liquid's effects on the treatment of skin cancer. For this purpose,

a numerical simulation of high-voltage pulse streamer discharge utilized for cancer medical therapy is investigated using COMSOL Multiphysics software. Pulse-source plasma energy transfer is optimized based on voltage, pressure, input power, total energy, pulse frequency, and flow rate. Results show that the electron energy and electric field can transiently reach greater levels than in stationary discharges. Over many pulses, O_3 and NO accumulate in the gas, while other neutral species are consumed. At the surface liquid, RONS accumulate and then decay after the plasma period. As voltage increases, reactive species densities increase due to higher power deposition. The streamer discharge improves with increasing electrode separation. Pressure decreases the ionizing front's propagation velocity. As a result, increased pressure decreases the number and the volume of streamer branches. Increasing the flow rate of N_2 gas reduces the cell death rate and decreases the efficiency of removing microorganisms by generating fewer reactive species. Another control mechanism is the pulse repetition frequency, and a higher pulse frequency increases the temperature of the active medium.

Because ROS and RNS have different timescales, gas flow can regulate the relative rates of ROS and RNS solvation into liquids. The gas flow rate increases while RNS in the liquid decreases. Degradation efficiency does not improve beyond a certain gas flow rate, and NO concentration at the system outlet decreases. The most likely cause of melanoma cell death is the water vapor reactive species like OH . As oxygen-derived reactive species, NO and O have a less significant effect and highlight the significance of the movement of water vapor from the surface into the culture medium.

Compared to necrosis, which occurs immediately to remove melanoma cells, plasma treatment causes cells to undergo apoptosis, resulting in cell death over hours or days, and survival rates do not decline quickly after treatment. Although chemical radiation therapy provides faster results in removing melanoma cells, plasma medicine, considering both long-lived and short-lived reactive species, demonstrates its ability to remove cancer cells while promoting tissue regeneration.

Data availability statement

The original contributions presented in the study are included in the article; further inquiries can be directed to the corresponding author.

Author contributions

SE: conceptualization, data curation, formal analysis, funding acquisition, methodology, project administration, resources, validation, and writing – original draft. NA: conceptualization, data curation, formal analysis, methodology, and writing – review and editing. EM: formal analysis, investigation, and writing – review and editing. SG: data curation, software, and writing – review and editing.

Funding

The author(s) declare that financial support was received for the research and/or publication of this article. This research project was funded by the Deanship of Scientific Research and Libraries, Princess Nourah bint Abdulrahman University, through the Program of Research Project Funding After Publication, grant No (RPFAP-65- 1445).

Conflict of interest

The authors declare that the research was conducted in the absence of any commercial or financial relationships that could be construed as a potential conflict of interest.

References

- O'Neill F, O'Neill L, Bourke P. Recent developments in the use of plasma in medical applications. *Plasma* (2024) 7, 284–99. doi:10.3390/plasma7020016
- Kazemi A, Nicol MJ, Bilén SG, Kirimanjswara GS, Knecht SD. Cold atmospheric plasma medicine: applications, challenges, and opportunities for predictive control. *Plasma* (2024) 7, 233–57. doi:10.3390/plasma7010014
- Koga-Ito CY, Kostov KG, Miranda FS, Milhan NVM, Azevedo Neto NF, Nascimento F, et al. Cold atmospheric plasma as a therapeutic tool in medicine and dentistry. *Plasma Chem Plasma Process* (2024) 44, 1393–429. doi:10.1007/s11090-023-10380-5
- Lavrikova A, Janda M, Bujdaková H, Hensel K. Eradication of single- and mixed-species biofilms of *P. aeruginosa* and *S. aureus* by pulsed streamer corona discharge cold atmospheric plasma. *Sci Total Environ* (2025) 959, 178184. doi:10.1016/j.scitotenv.2024.178184
- Hoffer P, Niedoba K, Jirásek V, Prukner V, Šimek M. Streamer-based discharge on water–air interface as a source of plasma-activated water: conceptual design and basic performance. *Plasma Chem Plasma Process* (2023) 43, 1531–47. doi:10.1007/s11090-023-10325-y
- Adesina K, Lin TC, Huang YW, Locmelis M, Han D. A review of dielectric barrier discharge cold atmospheric plasma for surface sterilization and decontamination. *IEEE Trans Radiat Plasma Med Sci* (2024) 8, 295–306. doi:10.1109/TRPMS.2024.3349571
- Ruirui G, Jiangling S, Jingshuo Z, Xinyi Z, Ni T, Fan R, et al. Investigation of the discharge characteristics of a nozzle-broadened plasma jet and its anticancer potential. *AIP Adv* (2025) 15, 035138. doi:10.1063/5.0251716
- Seong MJ, Park KR, Kim SJ, Joh HM, Moon H, Chung TH. Characterization and bacterial inactivation application of multiple pin-to-plate electrode-based DBD plasma driven by nanosecond-pulsed high voltage. *Phys Plasmas* (2025) 32, 023504. doi:10.1063/5.0241367
- Honda A, Inoue KI, Tamura S, Tanaka M, Wang Z, Tanaka T, et al. Effects of streamer discharge on PM2.5 containing endotoxins and polyaromatic hydrocarbons and their biological responses *in vitro*. *Int J Mol Sci* (2022) 23, 15891. doi:10.3390/ijms232415891
- Klenivskiy M, Khun J, Thonová L, Vaňková E, Scholtz V. Portable and affordable cold air plasma source with op-timized bactericidal effect. *Sci Rep* (2024) 14, 15930. doi:10.1038/s41598-024-66017-w
- Jinno R, Komuro A, Yanai H, Ono R. Antitumor abscopal effects in mice induced by normal tissue irradiation using pulsed streamer discharge plasma. *J Phys D: Appl Phys* (2022) 55, 17LT01. doi:10.1088/1361-6463/ac4c23
- Mizuno K, Yonetamari K, Shirakawa Y, Akiyama T, Ono R. Antitumor immune response induced by nanosecond pulsed streamer discharge in mice. *J Phys D: Appl Phys* (2017) 50, 12LT01. doi:10.1088/1361-6463/aa5d5b
- Walker RZ, Foster JE. Understanding the influence of fluid flow regime on plasma morphology and dose delivery at the plasma–liquid interface. *J Appl Phys* (2023) 133, 093301. doi:10.1063/5.0141059
- Seán K. *Generation and control of reactive species in low temperature atmospheric pressure plasma sources*. Dublin, Ireland: Dublin City University PhD Dissertation (2014).
- Zhuang C, Zeng R, Zhang B, He J. 2-D discontinuous galerkin method for streamer discharge simulations in Nitrogen. *IEEE T Magn* (2013) 49, 1929–32. doi:10.1109/TMAG.2013.2240669

Generative AI statement

The authors declare that no Generative AI was used in the creation of this manuscript.

Publisher's note

All claims expressed in this article are solely those of the authors and do not necessarily represent those of their affiliated organizations, or those of the publisher, the editors and the reviewers. Any product that may be evaluated in this article, or claim that may be made by its manufacturer, is not guaranteed or endorsed by the publisher.

- Liu Y, Korolov I, Trieschmann J, Steuer D, Gathen VS, Böke M, et al. Micro atmospheric pressure plasma jets excited in He/O₂ by voltage waveform tailoring: a study based on a numerical hybrid model and experiments. *Plasma Sourc Sci Technol* (2021) 30, 064001. doi:10.1088/1361-6595/abd0e0
- COMSOL AB. *COMSOL Multiphysics® v.5.1*. Stockholm, Sweden. Available online at: <http://www.comsol.com> (Accessed January 14, 2025) (2025).
- Neyts EC, Yusupov M, Verlactt CCW, Bogaerts A. Computer simulations of plasma–biomolecule and plasma–tissue interactions for a better insight in plasma medicine. *J Phys D: Appl Phys* (2014) 47, 293001. doi:10.1088/0022-3727/47/29/293001
- Wang M, Zhao JH, Tang MX, Li M, Zhao H, Li ZY, et al. Cell death modalities in therapy of melanoma. *Int J Mol Sci* (2025) 26, 3475. doi:10.3390/ijms26083475
- Mattia G, Puglisi R, Ascione B, Malorni W, Carè A, Matarrese P. Cell death-based treatments of melanoma: conventional treatments and new therapeutic strategies. *Cell Death Dis* (2018) 9, 112. doi:10.1038/s41419-017-0059-7
- Ajo P, Kornev I, Preis S. Pulsed corona discharge in water treatment: the effect of hydrodynamic conditions on oxidation energy efficiency. *Ind Eng Chem Res* (2015) 54, 7452–8. doi:10.1021/acs.iecr.5b01915
- Akiyama H, Akiyama M. Pulsed discharge plasmas in contact with water and their applications. *IEEE T Electr* (2020) 16, 6–14. doi:10.1002/tee.23282
- Buntat Z, Smith I, Razali N. Ozone generation by pulsed streamer discharge in air. *Appl Phys Res* (2009) 1, 1–10. doi:10.5539/apr.v1n2p2
- Choi J, Yamaguchi T, Yamamoto K, Namihira T, Sakugawa T, Katsuki S, et al. Feasibility studies of EMTP simulation for the design of the pulsed-power generator using MPC and BPFN for water treatments. *IEEE T Plasma Sci* (2006) 34, 1744–50. doi:10.1109/TPS.2006.883384
- Lietz AM, Kushner MJ. Air plasma treatment of liquid covered tissue: long timescale chemistry. *J Phys D: Appl Phys* (2016) 49, 425204. doi:10.1088/0022-3727/49/42/425204
- Ermolaeva SA, Varfolomeev AF, Chernukha MY, Yurov DS, Vasiliev MM, Kaminskaya AA, et al. Bactericidal effects of non-thermal argon plasma *in vitro*, in biofilms and in the animal model of infected wounds. *J Med Microbiol* (2011) 60, 75–83. doi:10.1099/jmm.0.020263-0
- Gershman S, Mozgina O, Belkind A, Becker K, Kunhardt E. Pulsed electrical discharge in bubbled water. *Contrib Plasma Phys* (2007) 46, 19–25. doi:10.1002/ctpp.200710004
- Elaiissi S, Charrada K. Simulation of cold atmospheric plasma generated by floating-electrode dielectric barrier pulsed discharge used for the cancer cell necrosis. *Coatings* (2021) 11, 1405. doi:10.3390/coatings11111405
- Gupta SB, Bluhm H. The potential of pulsed underwater streamer discharges as a disinfection technique. *IEEE T Plasma Sci* (2008) 36, 1621–32. doi:10.1109/TPS.2008.2001231
- Dijcks S, Kusýn L, Janssen J, Bilek P, Nijdam S, Hoder T. High-resolution electric field and temperature distributions in positive streamers. *Front Phys* (2023) 11, 1120284. doi:10.3389/fphy.2023.1120284
- Kolikova VA, Kurochkin VE, Paninac LK, Rutberga AF, Rutberga FG, Snetova VN, et al. Prolonged microbial resistance of water treated by a pulsed electrical discharge. *Tech Phys* (2007) 52, 263–70. doi:10.1134/S1063784207020193

32. Van Doremale ERW, Kondeti VSSK, Bruggeman PJ. Effect of plasma on gas flow and air concentration in the ef-fluent of a pulsed cold atmospheric pressure helium plasma jet. *Plasma Sourc Sci Technol* (2018) 27, 095006. doi:10.1088/1361-6595/aadb3
33. Kornev I, Saprykin F, Preis S. Stability and energy efficiency of pulsed corona discharge in treatment of dispersed high-conductivity aqueous solutions. *J Electrostat* (2017) 89, 42–50. doi:10.1016/j.elstat.2017.07.001
34. Janda M, Machala Z, Niklová A, Martišovič V. The streamer-to-spark transition in a transient spark: a dc-driven nanosecond-pulsed discharge in atmospheric air. *Plasma Sourc Sci Technol* (2012) 21, 045006. doi:10.1088/0963-0252/21/4/045006
35. Locke BR, Thagard SM. Analysis and review of chemical reactions and transport processes in pulsed electrical discharge plasma formed directly in liquid water. *Plasma Chem Plasma Process* (2012) 32, 875–917. doi:10.1007/s11090-012-9403-y
36. Lisitsyn IV, Nomiya H, Katsuki S, Akiyama H. Water treatment by pulsed streamer discharges. in: Proceedings of the Digest of Technical Papers, 12th IEEE International Pulsed Power Conference; Monterey, CA, United States (1999), 1, 468–71. doi:10.1109/PPC.1999.825512
37. Lu X, Pan Y, Liu K, Liu M, Zhang H. Spark model of pulsed discharge in water. *J Appl Phys* (2002) 91:24–31. doi:10.1063/1.1420765
38. Rodríguez Méndez BG, Callejas RL, Eguiluz RP, Cabrera AM, Valencia Alvarado R, Barocio SR, et al. Simulation study of a pulsed corona discharge by means an electrical model. in: *Proceedings of 6th EUROSIM congress on modeling and simulation*. Ljubljana, Slovenia (2007) 9–13.
39. Minamitani Y, Yamada T. Investigation of the influence of droplets to streamer discharge in water treatment by pulsed discharge in air spraying water droplets. *IEEE T Plasma Sci* (2016) 44, 2173–80. doi:10.1109/TPS.2016.2592515
40. Namihira T, Wang D, Katsuki S, Hackam R, Akiyama H. Propagation velocity of pulsed streamer discharges in atmospheric air. *IEEE T Plasma Sci* (2003) 31, 1091–4. doi:10.1109/TPS.2003.818765
41. Singha RK, Philipa L, Ramanujamb S. Continuous flow pulse corona discharge reactor for the tertiary treatment of drinking water: insights on disinfection and emerging contaminants removal. *Chem Eng J* (2019) 355, 269–78. doi:10.1016/j.cej.2018.08.109
42. Sugai T, Nguyen PT, Tokuchi A, Jiang W, Minamitani Y. The effect of flow rate and size of water droplets on the water treatment by pulsed discharge in air. *IEEE T Plasma Sci* (2015) 43, 3493–9. doi:10.1109/TPS.2015.2450741
43. Sugiarto AT, Ito S, Ohshima T, Sato M, Skalny JD. Oxidative decoloration of dyes by pulsed discharge plasma in water. *J Electrostat* (2003) 58, 135–45. doi:10.1016/S0304-3886(02)00203-6
44. Yan N, Wu Z, Tan T. Modeling of formaldehyde destruction under pulsed discharge plasma. *J Environ Sci Health* (2000) 35, 1951–64. doi:10.1080/10934520009377090
45. Chung KJ, Lee SG, Hwang YS, Kim CY. Modeling of pulsed spark discharge in water and its application to well cleaning. *Curr Appl Phys* (2015) 15, 977–86. doi:10.1016/j.cap.2015.05.010
46. Akishev Y, Balakirev A, Karalnik V, Petryakov A, Trushkin N. Numerical simulation of streamer spreading over the water surface. *J Phys: Conf Ser* (2019) 1328, 012061. doi:10.1088/1742-6596/1328/1/012061
47. Machala Z, Jedlovský I, Chládková L, Pongráč B, Giertl D, Janda M, et al. DC discharges in atmospheric air for bio-decontamination – spectroscopic methods for mechanism identification. *Eur Phys J D* (2009) 54, 195–204. doi:10.1140/epjd/e2009-00035-7
48. Doležalová E, Prukner V, Kuzminova A, Šimek M. On the inactivation of *Bacillus subtilis* spores by surface streamer discharge in humid air caused by reactive species. *J Phys D: Appl Phys* (2020) 53, 245203. doi:10.1088/1361-6463/ab7cf7
49. Timoshkin IV, Maclean M, Wilson MP, Given MJ, MacGregor SJ, Wang T, et al. Bactericidal effect of corona discharges in atmospheric air. *IEEE T Plasma Sci* (2012) 40, 2322–33. doi:10.1109/TPS.2012.2193621
50. Jang Sick P, Ihn H, Eun Ha C. Properties of plasma sterilizer using non-thermal atmospheric-pressure biocompatible plasma. *AIP Adv* (2019) 9, 075125. doi:10.1063/1.5096446
51. Kebriaei M, Ketabi A, Halvaei A. Pulsed corona discharge, a new and effective technique for water and air treatment. *Biol Forum– An Int J* (2015) 7, 1686–92. ISSN No. (Print): 0975-1130 ISSN No. (Online): 2249-3239.
52. Lisitsyn IV, Nomiya H, Katsuki S, Akiyama H. Streamer discharge reactor for water treatment by pulsed power. *Rev Sci Instrum* (1999) 70, 3457–62. doi:10.1063/1.1149937
53. Huiskamp T. Nanosecond pulsed streamer discharges Part I: generation, source-plasma interaction and energy-efficiency optimization. *Plasma Sourc Sci T* (2020) 29, 023002. doi:10.1088/1361-6595/ab53c5
54. Robert E. The role of electric fields in plasma treatment of cells. In: S. Bekeschus, T. Woedtke, editors. *Redox biology in plasma medicine*. 1st ed. Boca Raton: CRC Press 120–32. (2024). doi:10.1201/9781003328056
55. Ruma Lukes P, Aoki N, Spetlikova E, Hosseini SHR, Sakugawa T, Akiyama H, et al. Effects of pulse frequency of input power on the physical and chemical properties of pulsed streamer discharge plasmas in water. *J Phys D: Appl Phys* (2013) 46, 125202. doi:10.1088/0022-3727/46/12/125202
56. Bogaerts A, Yusupov M, Razzokov J, Van der Paal J. Plasma for cancer treatment: how can RONS penetrate through the cell membrane? Answers from computer modeling. *Front Chem Sci Eng* (2019) 13, 253–63. doi:10.1007/s11705-018-1786-8
57. Niyozaliev M, Matyakubov J, Abduvokhidov D, Attri P, Chen Z, Razzokov J. Unraveling the influence of nitration on pore formation time in electroporation of cell membranes: a molecular dynamics simulation approach. *J Phys D: Appl Phys* (2024) 57, 285202. doi:10.1088/1361-6463/ad3bc8
58. Abduvokhidov D, Yusupov M, Shahzad A, Attri P, Shiratani M, Oliveira MC, et al. Unraveling the transport properties of RONS across nitro-oxidized membranes. *Biomolecules* (2023) 13, 1043. doi:10.3390/biom13071043
59. Lu X, Naidis GV, Laroussi M, Reuter S, Graves DB, Ostrikov K. Reactive species in non-equilibrium atmospheric-pressure plasmas: generation, transport, and biological effects. *Phys Rep* (2016) 630, 1–84. doi:10.1016/j.physrep.2016.03.003
60. Al-rawaf AF, Khalaf TH. Simulation of positive streamer discharges in transformer oil. *J Phys: Conf Ser* (2022) 2322, 012066. doi:10.1088/1742-6596/2322/1/012066
61. Yagi I, Shirakawa Y, Hirakata K, Akiyama T, Yonemori S, Mizuno K, et al. Measurement of OH, O, and NO densities and their correlations with mouse melanoma cell death rate treated by a nanosecond pulsed streamer discharge. *J Phys D: Appl Phys* (2015) 48, 424006. doi:10.1088/0022-3727/48/42/424006
62. Biscop E, Baroen J, Backer JD, Berghe WV, Smits E, Bogaerts A, et al. Characterization of regulated cancer cell death pathways induced by the different modalities of non-thermal plasma treatment. *Cell Death Discov* (2024) 10, 416. doi:10.1038/s41420-024-02178-x
63. Arndt S, Wacker E, Li YF, Shimizu T, Thomas HM, Morfill GE, et al. Cold atmospheric plasma, a new strategy to induce senescence in melanoma cells. *Exp Dermatol* (2013) 22, 284–9. doi:10.1111/exd.12127
64. Namihira T, Yamaguchi T, Yamamoto K, Choi J, Kiyon T, Sakugawa T, et al. Characteristics of pulsed discharge plasma in water. in: Proceedings of 2005 IEEE Pulsed Power Conference; Monterey, CA, United States 1013–6. (2005). doi:10.1109/PPC.2005.300473